

## Droplet millifluidics for kinetic study of transketolase

A. Pinsolle,<sup>1</sup> F. Charmantray,<sup>2,3</sup> L. Hecquet,<sup>2,3,a)</sup> and F. Sarrazin<sup>1,b)</sup>

<sup>1</sup>Laboratory of the Future (LOF), SOLVAY/CNRS UMR 5258, 178 avenue du Docteur Schweitzer, F-33608 Pessac Cedex, France

<sup>2</sup>Université Clermont Auvergne, Université Blaise Pascal, Institut de Chimie de Clermont-Ferrand BP 10448, F-63000 Clermont-Ferrand, France

<sup>3</sup>CNRS, UMR 6296, ICCF, F-63171 Aubière, France

(Received 15 April 2016; accepted 18 October 2016; published online 10 November 2016)

We present a continuous-flow reactor at the millifluidic scale coupled with an online, non-intrusive spectroscopic monitoring method for determining the kinetic parameters of an enzyme, transketolase (TK) used in biocatalysis for the synthesis of polyols by carboligation. The millifluidic system used is based on droplet flow, a well-established method for kinetic chemical data acquisition. The TK assay is based on the direct quantitative measurement of bicarbonate ions released during the transketolase-catalysed reaction in the presence of hydroxypyruvic acid as the donor, thanks to an irreversible reaction: bicarbonate ions react with phosphoenolpyruvate (PEP) in the presence of PEP carboxylase as the first auxiliary enzyme. The oxaloacetate formed is reduced to malate by NADH in the reaction catalysed by malate dehydrogenase as the second auxiliary enzyme. The extent of oxidation of NADH was measured by spectrophotometry at 340 nm. This system gives a direct, quantitative, generic method to evaluate the TK activity versus different substrates. We demonstrate the accuracy of this strategy to determine the enzymatic kinetic parameters and to study the substrate specificity of a thermostable TK from thermophilic microorganism *Geobacillus stearothermophilus*, offering promising prospects in biocatalysis. Millifluidic systems are useful in this regard as they can be used to rapidly evaluate the TK activity towards various substrates, and also different sets of conditions, identifying the optimal operating environment while minimizing resource consumption and ensuring high control over the operating conditions. *Published by AIP Publishing.* [<http://dx.doi.org/10.1063/1.4966619>]

### INTRODUCTION

Biocatalysis has seen a rapid development in the past century, during which time many new technologies have been applied to broaden its use. Because of the high catalytic efficiency, substrate specificity and product stereoselectivity of biocatalysts, together with their environment-friendliness, biocatalytic processes have been tending to replace the conventional chemical synthesis in pharmaceutical,<sup>1</sup> fine chemical,<sup>2</sup> materials,<sup>3</sup> energy<sup>3</sup> and environment protection<sup>3</sup> industries. These processes require much work to optimize the conversion and product yield. Millifluidic reactors can be used to optimize reactions through the enhancement of heat and mass transfers, but our purpose in the present work was to construct a miniaturized system for the measurement of kinetic parameters and to find optimized reaction conditions for further applications in biocatalysis. Millifluidic systems are useful in this regard as they can be used to rapidly evaluate different sets of conditions and kinetic parameters, identifying the optimal operating environment while minimizing resource consumption and ensuring very good control over operating conditions.<sup>4</sup>

<sup>a)</sup>laurence.hecquet@univ-bpclermont.fr

<sup>b)</sup>flavie.sarrazin@solvay.com

Transketolase (TK), a thiamine diphosphate (ThDP)-dependent enzyme, has been shown to be a useful biocatalyst that stereospecifically forms a new carbon-carbon bond between a ketol group from a donor substrate and an aldehyde acceptor. For applications in biocatalysis, lithium hydroxypyruvate (HPA) is used as the donor substrate because the reaction becomes irreversible by the decarboxylation of HPA and the release of bicarbonate ions. Since TKs from different microbial sources can accept a wide range of hydroxylated and non-hydroxylated aliphatic,<sup>4-7</sup> and cyclic and aromatic aldehydes,<sup>4,8</sup> they represent a highly attractive biocatalytic platform technology for the synthesis of chiral polyols, (3*S*)-ketoses, with an ever-increasing range of applications<sup>8-12</sup> (Fig. 1). The millifluidic technology applied to TK-catalysed carbon-carbon bond formation reactions is of fundamental utility<sup>13-15</sup> in optimizing the reaction conditions. Several assay formats have been developed to probe the substrate tolerance of TK by measuring the remaining substrate or product formed. Measurement of chiral product formation by an optical method<sup>16,17</sup> is highly dependent on the substrate structure, and so not of generic utility. Determination of HPA depletion by near-UV spectroscopic monitoring<sup>18</sup> or HPLC (High Performance Liquid Chromatography) analysis<sup>14-20</sup> is hampered by low sensitivity or low throughput. Colorimetric determination of ketose formation with tetrazolium red-based oxidation is restricted to non-hydroxylated aldehyde acceptors such as propanal.<sup>16</sup> A major disadvantage of all methods that involve substrate/product determination is that they are often discontinuous, and do not allow direct measurement of enzyme kinetics. We have recently described an assay, independent of the substrate and the product, and based on direct monitoring of pH changes with phenol red as pH indicator.<sup>21</sup> In the TK catalytic reaction with HPA as the donor, one equivalent of bicarbonate is produced during HPA decarboxylation, raising the pH. Phenol red exposed to alkali changes colour from yellow to bright red.

Here we describe a novel TK assay method based on the direct quantitative measurement of bicarbonate ions reacting with phosphoenolpyruvate (PEP) in the presence of PEP carboxylase (PEPC). The oxaloacetate formed is reduced to malate by NADH in the reaction catalysed by malate dehydrogenase (MDH). The extent of oxidation of NADH is measured by spectrometry at 340 nm (Fig. 1). We combine a droplet-based continuous-flow reactor at millifluidic scale with an online, non-intrusive spectroscopic monitoring method. In the millifluidic reactor, droplets of reactants are generated as individual micro-batch reactors, and flow along a capillary. This offers four main advantages for the quantification of enzymatic kinetics:

- (i) Concentration of the substrate can be continuously varied while keeping all the other concentrations constant (enzyme, co-factors, etc.).
- (ii) A droplet-based millifluidic set-up is convenient to monitor the kinetic parameters, as already demonstrated in several fields of chemistry.<sup>22-25</sup> The reaction starts only when the droplets form: this sets the initial time of the reaction, which takes place continuously throughout the reactor so that each length of reactor tube corresponds to a time of reaction (time-distance equivalence).<sup>22,26</sup> Hence all reaction times (even very short ones) can be analysed at any time using an online probe placed after the formation of the droplets. For

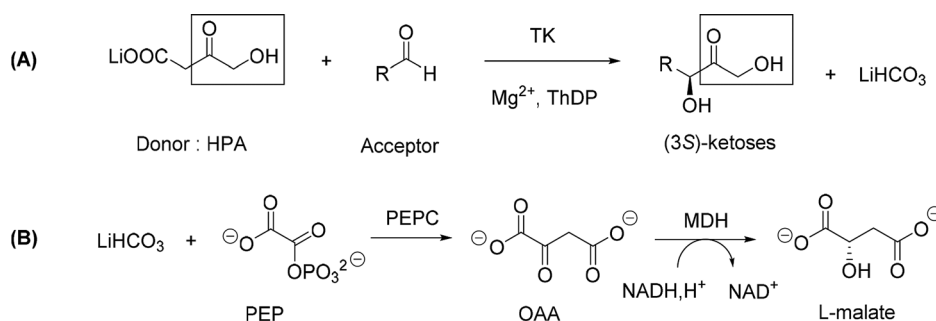


FIG. 1. Principle of the bicarbonate assay method for TK activity determination. (a) Reaction catalysed by TK. (b) Auxiliary enzymatic system.

this purpose, we chose a spectrometer probe that was non-intrusive, and could be easily moved along the entire tubing length.

- (iii) The millifluidic set-up is particularly accurate for the monitoring of short reaction times. Movements of recirculation occur inside the droplets owing to the forced convection induced by the contact of the walls of the tubing.<sup>27–29</sup> They enable a very short reactant mixing time, down to a few milliseconds in certain cases.<sup>28</sup> Thus the conditions (tube size, droplet velocity) can be chosen according to the reaction kinetics, in order to avoid its limitation by mass transfer. In the present study, the measured reaction times were between 1 and 10 min, and the mixing time less than 1 min.
- (iv) The statistics of the results are robust, as each experimental point (one time, one concentration) is acquired on several tens of droplets. As a result, each initial rate is extracted from hundreds of individual batch experiments. This is of great importance for the accuracy of the linear regression of the Lineweaver-Burk model performed later. The number of repetitions must be high because the slope of the Lineweaver-Burk linear regression depends on each point, and a small change in this slope can drastically affect  $K_m$ .

We demonstrate the application of the millifluidic system and of the online generic method to the TK-catalysed reaction in terms of kinetic parameters and substrate affinity. A TK from the thermophilic microorganism *Geobacillus stearothermophilus* was used, which will be useful for future biocatalyst development.<sup>21</sup> From the industrial point of view, enzymatic processes at elevated temperatures offer many advantages, such as higher reaction rates, and better tolerance of organic solvents. We showed that TK<sub>gst</sub> offers several advantages: (i) TK<sub>gst</sub> is thermostable and retained 100% activity for one week at 50 °C, (ii) the relative velocity of TK<sub>gst</sub> catalysis at 50 °C was 8 times higher than at 20 °C,<sup>21</sup> and (iii) the high stability of TK<sub>gst</sub> in the presence of co-solvents such as organic solvents, but also ionic liquids, can be used to improve the solubility of acceptor substrates. We showed that TK<sub>gst</sub> activity was stable for 16 h in the aqueous solution containing 30%–50% [BMIm][Cl] enhancing TK<sub>gst</sub> activity towards pentoses, particularly D-ribose.<sup>13</sup>

## MATERIALS AND METHODS

### Reactants

Unless otherwise stated, all chemicals and reagents (Sigma-Aldrich) were used without further purification. Purified TK from a thermophilic microorganism, *Geobacillus stearothermophilus* (TK<sub>gst</sub>), was used. It was obtained by a protocol described elsewhere.<sup>21</sup>

Each solution was prepared fresh in glycylglycine buffer solution (100 mM, pH 7.5) except for HPA (Sigma Aldrich) stock solution, which was prepared in glycylglycine buffer solution (100 mM, pH 7).

### Millifluidic reaction

We used a millifluidic device to generate droplets containing the reactants and the catalyst, which were carried by inert oil. We describe below the technical details of the injection stage for generating drops and initiating the reaction, and the serpentine tubing in which the reaction takes place (Fig. 2).

### Injection

All the reactants were stored in glass syringes (25 ml for the oil phase S6, 1 ml for the catalyst S2 and 2.5 ml for the other reagents) and injected at a controlled flow rate by means of six syringe-pump modules (Nemesys, Cetoni) in the conditions described in Table I. These syringes enabled us to tune the glycolaldehyde (GA) or other aldehyde and HPA concentrations separately, while keeping all the other concentrations constant. In this way, the concentrations of the solutes were chosen such that they would be diluted as follows, once combined in the droplets: 0.05 mg ml<sup>−1</sup> TK<sub>gst</sub>, 2 mM thiamine diphosphate (ThDP), 1.5/3.1/6.2/12.5/25 mM of HPA

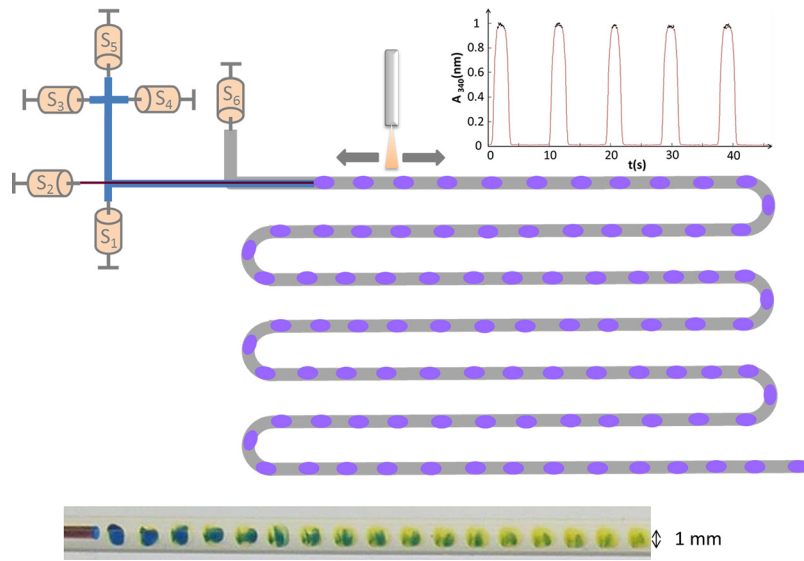


FIG. 2. Top: Schematic view of the microfluidic device. Bottom: Depiction of the droplet formation at the concentric junction; droplets are separated by inert fluorinated oil; a colour indicator was used to visualize how the fluids mix inside the droplets.

with 25 mM GA and 3.1/6.2/12.5/25 mM of GA with 25 mM HPA (depending on the experiments). The concentrations of the solutes from the auxiliary system were 4 mM for PEP, PEPC 5 U ml<sup>-1</sup>; MDH 5 U ml<sup>-1</sup> and 2.5 mM NADH.

All the injection tubes (inner diameter 1/32 in., outer diameter) 1/16 in. were connected to the syringes by Luer lock connectors (Upchurch). All the tubes were made of perfluoroalkoxy polymer (PFA) (Idex) and had different diameters. As shown in Fig. 2, syringes 1, 3, 4, and 5

TABLE I. Detailed content of the syringes and flow rates, and their impact on the final concentration inside the droplets, which serves as individual batch reactors. Abbreviations: phosphoenolpyruvate (PEP), PEP carboxylase (PEPC), malate dehydrogenase (MDH), reduced nicotinamide dinucleotide (NADH), transketolase (TK<sub>gst</sub>), thiamine diphosphate (ThDP), lithium hydroxypyruvate (HPA), glycolaldehyde (GA), glycylglycine (gly-gly).

Syringe: reagents	Concentration		Flow rate (μl/h)
	In syringe	In droplet	
S1			
PEP (mM)	8.8	4	205
PEPC (U ml <sup>-1</sup> )	11	5	
MDH (U ml <sup>-1</sup> )	11	5	
NADH (mM)	5.5	2.5	
S2			
TK <sub>gst</sub> (mg ml <sup>-1</sup> )	0.45	0.05	50
ThDP (mM)	18	2	
S3			
HPA (mM)	112.5	3.1–25	12.5–100
S4			
GA (mM)	112.5	1.5–25	6–100
S5			
Buffer pH 7.5 gly-gly (mM)	100		94–0
Perfluorodecalin			1600

(reactants and auxiliary enzymes) were eventually connected to the same tubing (inner diameter  $500\ \mu\text{m}$  and outer diameter  $1/32\ \text{in.}$ , blue in the figure). The length of this tube ( $30\ \text{cm}$ ) was chosen so that all the components had time to mix by diffusion. Via a T-junction, a smaller tube (inner diameter  $150\ \mu\text{m}$  and outer diameter  $360\ \mu\text{m}$ , red in the figure) which contained the  $\text{TK}_{\text{gst}}$  (from syringe S2) was inserted inside the previous one until the droplets formed. In this way, the catalyst TK and ThDP came into contact with all the other aqueous components at the time of droplet formation, which therefore set the initial time of the reaction.

### Serpentine

The drops formed at a concentric junction where the reactants met an inert carrier phase (perfluorodecalin, ABC). The drops (volume  $0.5\ \mu\text{l}$ ) then flowed inside the PFA capillary tubing of inner diameter  $1\ \text{mm}$  (outer diameter  $1/16\ \text{in.}$ ) at a constant velocity of  $0.73\ \text{mm/s}$  (see picture in Fig. 2). The reaction tubing was  $80\ \text{cm}$  in length. In this tube, flow was laminar ( $\text{Re} < 0.15$ ). As illustrated in the scheme of Figure 2, six bends were placed along the flow path. Their radius curvature ( $0.8\ \text{cm}$ ) was chosen so that the bends did not disturb the droplet flow, which was verified visually (picture of the flow remained the same all along the tube) and spectrometrically (conservation of droplet signal frequency). Previous studies in these conditions have estimated the mixing time to be less than  $1\ \text{min}$  according to the inner diameter of the tube and the droplet velocity.<sup>23,30</sup> Indeed, in first approximation, the mixing time inside the droplets is equal to the diffusion time over the quarter of the tube diameter.

The reaction tubing was inserted into an aluminium plate ( $12 \times 12 \times 0.8\ \text{cm}^3$ ) in contact with a Peltier regulator, which allowed the reaction temperature to be controlled. Indeed, as described elsewhere,<sup>31,32</sup> as PFA is a good thermal insulator ( $\lambda = 0.25\ \text{W M}^{-1}\text{K}^{-1}$ ) and aluminium an excellent thermal conductor ( $\lambda = 237\ \text{W M}^{-1}\text{K}^{-1}$ ), the outer temperature of the tube is set by one of the aluminium plates, and heat transfer into air is negligible. Eventually, the small size of the tubing permits fast homogenization of internal temperature and optimum evacuation of calories.

### Reaction monitoring

The thermostated millifluidic system was placed in the centre of an adjustable  $x,y,z$ -axis micrometer table on which the fibre-optics system was fixed. We used an FCR, 7UV200 reflection probe (Avantes). The light from a 43668 light source (Avantes) was sent through six illumination fibres to the sample, and the reflection was measured by a seventh fibre in the centre of the reflection probe tip. The seventh fibre was coupled to an AvaSpec 43668 spectrometer (Avantes) configured to the appropriate wavelength of interest ( $340\ \text{nm}$ ). The activity of the enzyme was determined by determining one of the products formed by the TK reaction, namely, the bicarbonate ions  $\text{HCO}_3^-$ . Bicarbonate quantification<sup>33</sup> allowed us to link, at each time, the TK activity to the rate of NADH oxidation, measured at  $340\ \text{nm}$ . There is an equimolar relation between the product formation (ketoses and bicarbonate) and NADH consumption. We thus obtained the following relation:

$$[\text{NADH}]_{\text{m}} = [\text{NADH}]_0 - [\text{HCO}_3^-], \quad (1)$$

where  $[\text{NADH}]_{\text{m}}$  was the concentration of NADH measured at each time in the droplet,  $[\text{NADH}]_0$  was the initial concentration of NADH in the droplet, and  $[\text{HCO}_3^-]$  was the concentration of  $\text{HCO}_3^-$  produced by the TK reaction.

Two parameters were previously checked. First we determined the linearity domain for the NADH signal. A calibration curve (data not shown) was measured at  $340\ \text{nm}$ , which showed the correct linearity for NADH concentration range up to  $2.5\ \text{mM}$ . Second, the relationship between the quantity of  $\text{HCO}_3^-$  produced during the TK reaction and the absorbance of the NADH indicator was determined by titration of the entire  $\text{TK}_{\text{gst}}$  assay mixture with  $\text{HCO}_3^-$  with all elements included, but omitting the aldehyde substrate to exclude catalytic turnover. A control calibration curve (data not shown) was plotted with a variation of the  $\text{HCO}_3^-$

concentration in the droplet from 0 to 2.5 mM, mimicking the increase in  $\text{HCO}_3^-$  during the  $\text{TK}_{\text{gst}}$  catalytic reaction. At the time of post-treatment, we calculated absorbance versus time by taking the reference intensity in the continuous phase. We thus obtained a rectangular waveform in which the step height was proportional to the NADH concentration inside the droplets (see signal example in Fig. 2). One advantage of the system is that each spectroscopic measurement is made on 30 identical droplets. For a kinetic measurement where  $n$  measures are made along the tubing, the kinetic curve is obtained from  $30n$  different reactors, which significantly improves the statistics of the data in comparison with classical techniques, where one kinetic curve corresponds to one reactor. The calibration was done for several compositions of NADH on hundreds of droplets, and gave a precision of 10%.

## RESULTS

### Kinetic parameters determination

In the millifluidic device, droplets contain the reactants and the catalyst, and are carried by inert oil. One advantage of the droplet-based approach is the equivalence between the position of the droplet in the channel, and the reaction time: i.e., according to the rate of the reaction, all the droplets have the same chemical composition when they reach the same position along the channel. By using non-intrusive spectrophotometric technique across the wall of the channels, concentrations at any time of the reaction can be determined. This strategy lets us quantify bicarbonate ions<sup>34</sup> and link, at each time, the TK activity to the rate of NADH oxidation, measured at 340 nm. The accuracy of kinetic rate constants for enzymatic reactions requiring a series of experiments at different substrate concentrations in a well-mixed and temperature-controlled container, the millifluidic approach offers reliability, repeatability, and reproducibility for *in situ* investigation of enzymatic kinetic parameters.

The kinetic constants were determined by varying the concentration of the individual substrate (GA or HPA) while keeping all other parameters constant. Initial velocity rates were measured for all those conditions in a large number of droplets (Figs. 3(a) and 4(a)). The resulting kinetic parameters  $v_{\text{max}}$  and  $K_m$  could be calculated from the linear regressions obtained for the two substrates, GA and HPA, using Michaelis-Menten model and Lineweaver-Burk regression<sup>35,36</sup> (Figs. 3(b) and 4(b)).

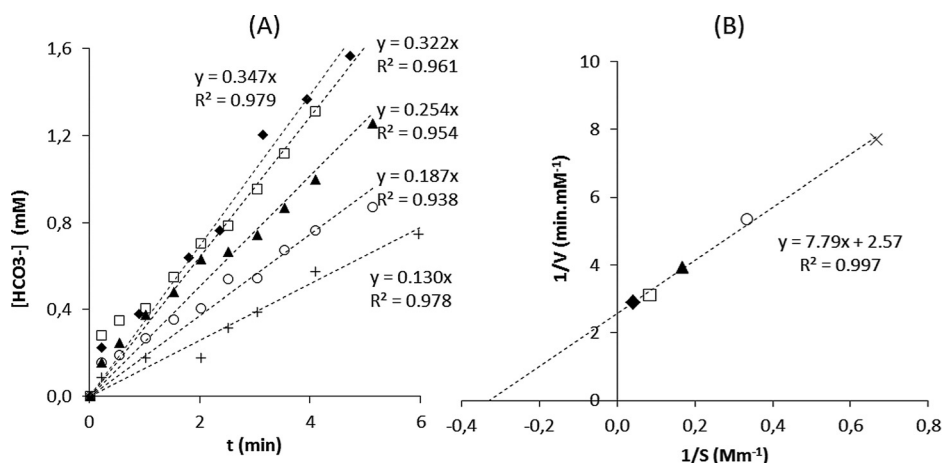


FIG. 3. (a) Determining the initial velocity. The amount of product formed at different HPA concentrations (+ 1.5 mM,  $\circ$  3 mM,  $\blacktriangle$  6 mM,  $\square$  12 mM and  $\blacklozenge$  25 mM) was plotted against time. Experiments were conducted at 35 °C with 25 mM GA, 0.05  $\text{mg ml}^{-1}$   $\text{TK}_{\text{gst}}$ , 2 mM ThDP. The concentrations of the solutes from the auxiliary system were 4 mM for PEP, PEPC/MDH 5 U  $\text{ml}^{-1}$  and 2.5 mM NADH. The initial velocity ( $v_0$ ) for each GA concentration was determined from the slope of the curve. (b) Determining the kinetic constant  $K_m$  and  $v_{\text{max}}$  by Lineweaver-Burk plot. This linear regression integrates 1290 individual batch condition results.



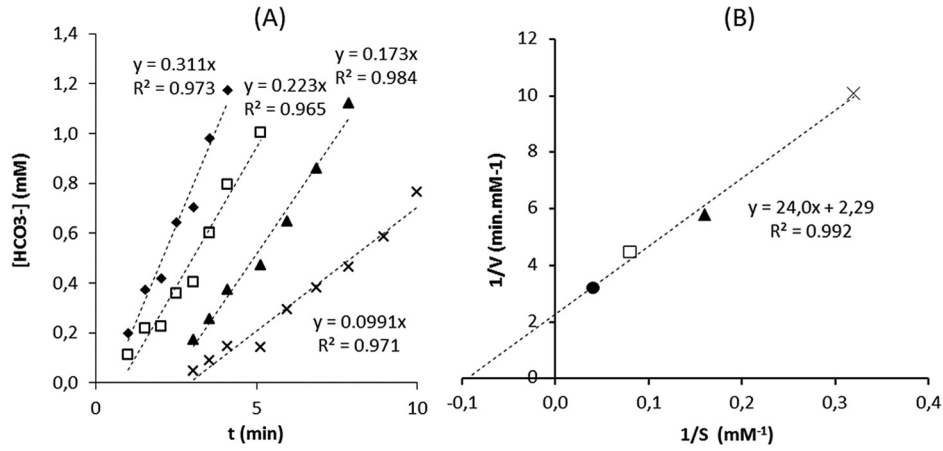


FIG. 4. (a) Determining the initial velocity. The amount of product formed at different GA concentrations ( $\times$  3 mM,  $\blacktriangle$  6 mM,  $\square$  12 mM and  $\blacklozenge$  25 mM) was plotted against time. Experiments were conducted at 35 °C with 25 mM HPA, 0.05 mg ml $^{-1}$  TK<sub>gst</sub>, 2 mM ThDP. The concentrations of the solutes from the auxiliary system were 4 mM for PEP, PEPC/MDH 5 U ml $^{-1}$  and 2.5 mM NADH. The initial velocity ( $v_0$ ) for each GA concentration was determined from the slope of the curve. (b) Determining kinetic constant  $K_m$  and  $v_{\max}$  by Lineweaver-Burk plot. This linear regression integrates 930 individual batch condition results.

The kinetic parameter results are summarized in Table II. We find a  $v_{\max}$  value of 0.45 mM min $^{-1}$  (9 U mg $^{-1}$ ) from the GA variation experiments, and 0.38 mM min $^{-1}$  (7.6 U mg $^{-1}$ ) from the HPA experiments.

For the aldehydic acceptor components (GA), the  $K_m$  value of 11.1 mM determined with TK<sub>gst</sub> was close to the published value (14 mM) with *E. coli* TK and 50 mM HPA as the donor.<sup>39</sup> Higher values (35 mM and 200 mM) were measured in the presence of wild type *E. coli* TK and mutant TK, respectively.<sup>37</sup>

For HPA, the  $K_m$  value of 2.92 mM determined with the TK<sub>gst</sub> was almost identical to the recently published value of 5.3 mM using an HPLC method<sup>37</sup> with 50 mM glycolaldehyde using wild type TK from *E. coli*. A similar value (4.78 mM) was found with a TK from *Plasmodium falciparum*.<sup>38</sup> A higher value for HPA was recorded (18 mM) by spectrophotometry using a phosphorylated acceptor with *E. coli* TK.<sup>39</sup>

In parallel,  $K_m$  values were measured in a classical batch reactor; they were 2.5 mM for HPA<sup>40</sup> and 10 mM for GA (not published), in agreement with the millifluidic results.

The data obtained from our online monitoring system were sufficiently reliable for rapid and direct quantitative comparison. The data were correlated with HPLC measurement at the output of the device, and for a set of HPA and GA concentrations, a difference of 10% in  $v_{\max}$  was found.

Statistical analysis of the data also gives an estimate of the representativeness of the data. This analysis includes the error on the calibration, the error on the initial velocity determination and the error on each plot in the Lineweaver-Burk model. For HPA concentration variation, the 95% self confidence regression gives the following results (Fig. 5):

- $1/v_{\max} = 2.63 \pm 0.35 \text{ min mM}^{-1}$ , which gives  $v_{\max} = 0.38 \pm 0.05 \text{ mM min}^{-1}$
- $1/K_m = 0.343 \pm 0.010 \text{ mM}^{-1}$ , which gives  $K_m = 2.92 \pm 0.08 \text{ mM}$ .

It is noteworthy that 1290 individual droplets served for the analysis of these results.

TABLE II. Kinetic parameters of the best acceptor glycolaldehyde and of the donor substrate HPA obtained from Figs. 3 and 4.

	$v_{\max}$ (mM min $^{-1}$ )	$K_m$ (mM)
Acceptor substrate: GA	$0.45 \pm 0.20$	$11.1 \pm 3.70$
Donor substrate: HPA	$0.38 \pm 0.05$	$2.92 \pm 0.08$

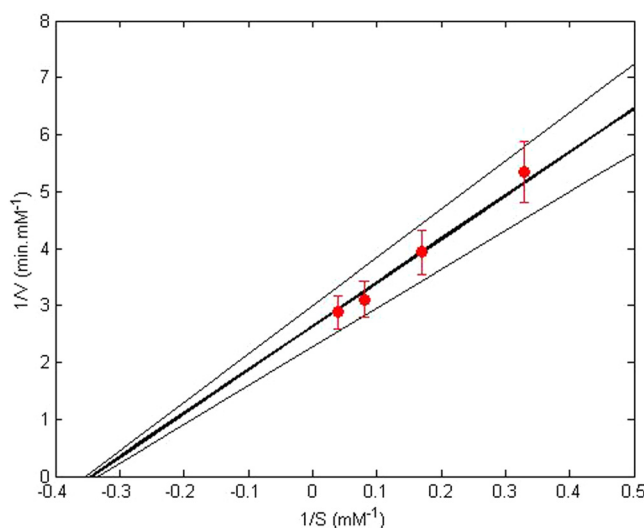


FIG. 5. Lineweaver-Burk plot for HPA concentration variation with 95% confidence area. The error bars integrate the error in the acquisition of each initial velocity value (error on calibration and repetition of the acquisition in hundreds of droplets).

The same statistic calculation was done on data from Fig. 4 and gave results on GA kinetic parameters which are given in Table II.

### Determination of TK acceptor specificity

The assay method was developed as a way to determine the catalytic potency of the  $\text{TK}_{\text{gst}}$  under identical reaction conditions for direct comparison towards various acceptor aldehydes. For each substrate, around 250 individual droplets were analysed for the extraction of the velocity rates. Polyhydroxyaldehydes (**1–3**) and linear aliphatic aldehydes (**4–6**) were selected to determine the influence of chain length on  $\text{TK}_{\text{gst}}$  reaction velocity. The results are given in Table III.

Several authors have contributed to the determination of the substrate specificity of TK enzymes from different sources (*E. coli*, *S. cerevisiae*, *G. stearothermophilus*) using different assay methods towards various phosphorylated and unphosphorylated aldoses or aldehydes.<sup>4,14–20</sup> The activity profiles of TKs are very similar, owing to the strong homology of active sites. Our system yields the same results as those obtained with  $\text{TK}_{\text{gst}}$  using other methods. Polyhydroxylated substrates give higher rates. GA is the best acceptor, followed by D-erythrose and D-ribose. TK has been found to tolerate some non- $\alpha$ -hydroxylated aldehydes,

TABLE III. Determination of  $\text{TK}_{\text{gst}}$  acceptor specificity versus glycolaldehyde (reference), non- $\alpha$ -hydroxylated aliphatic aldehydes, and  $\alpha$ -hydroxylated aldehydes. The assays were run at 35 °C with 25 mM HPA and 25 mM of various aldehydes, 0.05 mg ml<sup>−1</sup>  $\text{TK}_{\text{gst}}$ , 2 mM ThDP. The concentrations of the solutes from the auxiliary system were 4 mM for PEP, PEPC/MDH 5 U ml<sup>−1</sup> and 2.5 mM NADH.  $v_{\text{rel}}$  gives the proportional efficiency in comparison to the glycolaldehyde as a substrate.

		$v_o$ (U mg <sup>−1</sup> )	$v_{\text{rel}}$ (%)
1	Glycolaldehyde (C <sub>2</sub> )	6.2	100
2	D-Erythrose (C <sub>4</sub> )	2.6	41
3	D-Ribose (C <sub>5</sub> )	2.2	35
4	Butyraldehyde (C <sub>4</sub> )	1.7	26
5	Valeraldehyde (C <sub>5</sub> )	1.0	17
6	Isovaleraldehyde (C <sub>5</sub> )	1.1	18



but compared with  $\alpha$ -hydroxylated aldehyde, lower substrate activities were reported.<sup>41</sup> For the aliphatic non- $\alpha$ -hydroxylated series, we observed a drastic decrease in the TK reaction velocities.

## CONCLUSION

We demonstrate the efficiency of a droplet-based continuous-flow reactor at the millifluidic scale coupled with an online, non-intrusive spectroscopic monitoring method for the determination of kinetic parameters of an enzyme, TK<sub>gst</sub>. We developed an appropriate multienzymatic TK assay based on the direct quantitative measurement of bicarbonate ions released by the TK reaction. This strategy offers an efficient, sensitive, and rapid way to evaluate TK<sub>gst</sub> activities and kinetic parameters. The latter are obtained by initial rate measurements, which are particularly accurate in our system owing to mixing time and temperature control. Besides its online analysis and miniaturization aspects, our method provides statistic data, and so is particularly accurate for feeding models with linear regression and linearization processes such as the Lineweaver-Burk one. This coupled system could be applied to other enzymatic or chemical reactions with formation of bicarbonate ions. Our strategy offers promising prospects for identifying different sets of conditions and optimal operating environments, while minimizing resource consumption.

## ACKNOWLEDGMENTS

This work was supported by the French National Research Agency (ANR Nanocausys). LOF authors gratefully acknowledge Cindy Hany, Jacques Leng, and Pierre Guillot for their help. ICCF authors thank PhD student Marion Lorillière for the preparation of purified TK<sub>gst</sub>.

- <sup>1</sup>M. Schedel, *Chem. Ing. Tech.* **78**, 485 (2006).
- <sup>2</sup>W. J. W. Watson, *Green Chem.* **14**, 251 (2012).
- <sup>3</sup>M. Philippe, B. Didillon, and L. Gilbert, *Green Chem.* **14**, 952 (2012).
- <sup>4</sup>E. G. Hibbert, T. Senussi, M. E. Smith, S. J. Costelloe, J. M. Ward, H. C. Hailes, and P. A. Dalby, *J. Biotechnol.* **134**, 240 (2008).
- <sup>5</sup>C. Chang, J. Sustarich, R. Bharadwaj, A. Chandrasekaran, P. D. Adamsand, and A. K. Singh, *Lab Chip* **13**, 1817 (2013).
- <sup>6</sup>A. Cázares, J. L. Galman, L. G. Crago, M. E. Smith, J. Strafford, L. Ríos-Solís, G. J. Lye, P. A. Dalby, and H. C. Hailes, *Org. Biomol. Chem.* **8**, 1301 (2010).
- <sup>7</sup>D. Yi, S. Thangavelu, T. Devamani, F. Charmantray, L. Hecquet, and W.-D. Fessner, *Chem. Commun.* **51**, 480 (2015).
- <sup>8</sup>J. Abdoul Zabar, M. Lorillière, D. Yi, T. Saravanan, T. Devamani, L. Nauton, F. Charmantray, V. Hélaine, W.-D. Fessner, and L. Hecquet, *Adv. Synth. Catal.* **357**, 1715 (2015).
- <sup>9</sup>P. Payongsri, D. Steadman, J. Strafford, A. Mac Murray, H. C. Hailes, and P. A. Dalby, *Org. Biomol. Chem.* **10**, 9021 (2012).
- <sup>10</sup>R. Wohlgemuth, *J. Mol. Catal. B: Enzym.* **61**, 23 (2009).
- <sup>11</sup>F. Charmantray, V. Hélaine, B. Legeret, and L. Hecquet, *J. Mol. Catal. B: Enzym.* **57**, 6 (2009).
- <sup>12</sup>A. Ranoux, S. K. Karmee, J. Jin, A. Bhaduri, A. Caiazzo, I. W. C. E. Arends, and U. Hanefeld, *ChemBioChem* **13**, 1921 (2012).
- <sup>13</sup>G. Ali, T. Moreau, C. Forano, C. Mousty, V. Prevot, F. Charmantray, and L. Hecquet, *ChemCatChem* **7**, 3163 (2015).
- <sup>14</sup>J. Sukumaran and U. Hanefeld, *Chem. Soc. Rev.* **34**, 530 (2005).
- <sup>15</sup>J. Lawrence, B. O'Sullivan, G. J. Lye, R. Wohlgemuth, and N. Szita, *J. Mol. Catal. B: Enzym.* **95**, 111 (2013).
- <sup>16</sup>M. E. B. Smith, U. Kaulmann, J. M. Ward, and H. C. Hailes, *Bioorg. Med. Chem.* **14**, 7062 (2006).
- <sup>17</sup>G. A. Kochetov, R. A. Usmanov, and A. T. Mevkh, *Anal. Biochem.* **88**, 296 (1978).
- <sup>18</sup>I. A. Sevostyanova, O. N. Solovjeva, and G. A. Kochetov, *Biochemistry (Moscow)* **71**, 560 (2006).
- <sup>19</sup>G. A. Kochetov and P. P. Filippov, *Anal. Biochem.* **48**, 286 (1972).
- <sup>20</sup>O. J. Miller, E. G. Hibbert, C. U. Ingram, G. J. Lye, and P. A. Dalby, *Biotechnol. Lett.* **29**, 1759 (2007).
- <sup>21</sup>D. Yi, T. Devamani, J. Abdoul-Zabar, F. Charmantray, V. Helaine, L. Hecquet, and W. D. Fessner, *ChemBioChem* **13**, 2290 (2012).
- <sup>22</sup>H. Song, J. D. Tice, and R. F. Ismagilov, *Angew. Chem. Int. Ed.* **42**(7), 767 (2003).
- <sup>23</sup>N. Lorber *et al.*, *Lab Chip* **11**, 779 (2011).
- <sup>24</sup>K. Olivon and F. Sarrazin, *Chem. Eng. J.* **227**, 97 (2013).
- <sup>25</sup>French patents WO 2008/043860 and WO 2008/043922 (15 October 2007).
- <sup>26</sup>G. Cristobal, L. Arbouet, F. Sarrazin, D. Talaga, J.-L. Bruneel, M. Joanicot, and L. Servant, *Lab Chip* **6**(9), 1140 (2006).
- <sup>27</sup>F. Sarrazin, T. Bonometti, K. Loubière, L. Prat, C. Gourdon, and J. Magnaudet, *AIChE J.* **52**(12), 4061 (2006).
- <sup>28</sup>F. Sarrazin, L. Prat, N. Di Miceli, D. R. Link, G. Cristobal, and D. A. Weitz, *Chem. Eng. Sci.* **62**(4), 1042 (2007).
- <sup>29</sup>Z. B. Stone and H. A. Stone, *Phys. Fluids* **17**, 063103 (2005).
- <sup>30</sup>M. Romano, C. Pradere, F. Sarrazin, J. Toutain, and J. C. Batsale, *Chem. Eng. J.* **273**, 325 (2015).
- <sup>31</sup>C. Hany, C. Pradere, J. Toutain, and J. C. Batsale, *Quant. Infrared Thermogr. J.* **5**(2), 211 (2008).
- <sup>32</sup>M. Romano, C. Pradere, J. Toutain, C. Hany, and J. C. Batsale, *Quant. Infrared Thermogr. J.* **11**(2), 134 (2014).

- <sup>33</sup>J. Abdoul-Zabar, I. Sorel, V. Helaine, F. Charmantray, T. Devamani, D. Yi, V. Berardinis, D. Louis, P. Marliere, W. D. Fessner, and L. Hecquet, *Adv. Synth. Catal.* **355**, 116 (2013).
- <sup>34</sup>R. L. Forrester, L. J. Walaji, D. A. Silvermann, and K. J. Pierre, *Clin. Chem.* **22**(2), 243 (1976).
- <sup>35</sup>R. A. Copeland, *Enzymes: A Practical Introduction to Structure, Mechanism and Data Analysis* (Wiley-VCH, 2000).
- <sup>36</sup>D. Voet, J. G. Voet, and W. P. Pratt, *Fundamentals of Biochemistry* (John Wiley & Sons, Inc., 1999).
- <sup>37</sup>E. G. Hibbert, T. Senussi, S. J. Costelloe, W. Lei, M. E. B. Smith, J. M. Ward, H. C. Hailes, and P. A. Dalby, *J. Biotechnol.* **131**, 425 (2007).
- <sup>38</sup>S. Joshi, A. R. Singh, A. Kumar, P. C. Misra, M. I. Siddiqi, and J. K. Saxena, *Mol. Biochem. Parasitol.* **160**, 32 (2008).
- <sup>39</sup>G. A. Sprenger, U. Schörken, G. Sprenger, and H. Sahm, *Eur. J. Biochem.* **230**, 525 (1995).
- <sup>40</sup>M. Lorillière, M. De Sousa, F. Bruna, E. Heuson, T. Gefflaut, V. de Berardinis, T. Saravanan, D. Yi, W.-D. Fessner, F. Charmantray, and L. Hecquet, "One-pot, two-step cascade synthesis of naturally rare L-erythro (3S,4S) ketoses by coupling a thermostable transaminase and transketolase," *Green Chem.* (published online).
- <sup>41</sup>G. R. Hobbs, M. D. Lilly, N. J. Turner, J. N. Ward, A. J. Willets, and J. M. Woodley, *J. Chem. Soc., Perkin Trans. 1* **1993**, 165 (1993).